

Modeling and Design of RIS-Assisted Multi-cell Multi-band Networks with RSMA

Abdelhamid Salem, *Member, IEEE*, Kai-Kit Wong, *Fellow, IEEE*, Chan-Byoung Chae, *Fellow, IEEE*, and Yangyang Zhang

Abstract—Reconfigurable intelligent surface (RIS) has been identified as a promising technology for future wireless communication systems due to its ability to manipulate the propagation environment intelligently. RIS is a frequency-selective device, thus it can only effectively manipulate the propagation of signals within a specific frequency band. This frequency-selective characteristic can make deploying RIS in wireless cellular networks more challenging, as adjacent base stations (BSs) operate on different frequency bands. In addition, rate-splitting multiple access (RSMA) scheme has been shown to enhance the performance of RIS-aided multi-user communication systems. Accordingly, this work considers a more practical reflection model for RIS-aided RSMA communication systems, which accounts for the responses of signals across different frequency bands. To that end, new analytical expressions for the ergodic sum-rate are derived using the moment generating function (MGF) and Jensen's inequality. Based on these analytical sum-rate expressions, novel practical RIS reflection designs and power allocation strategies for the RSMA scheme are proposed and investigated to maximize the achievable sum-rate in RIS-assisted multi-cell, multi-band cellular networks. Simple sub-optimal designs are also introduced and discussed. The results validate the significant gains of our proposed reflection design algorithms with RSMA over conventional schemes in terms of achievable sum-rate. Additionally, the power allocation strategy for the RSMA scheme is shown to offer superior performance compared to conventional precoding schemes that do not rely on RSMA.

Index Terms—Reconfigurable intelligent surface, rate splitting multiple access, and zero forcing forcing.

I. INTRODUCTION

Reconfigurable intelligent surface (RIS) technology has been proposed recently to radically change and control the wireless propagation environment [1]–[4]. More specifically, RIS is a meta-surface composed of low-cost passive reflecting elements, and each element can be controlled to adjust the phase shift and amplitude of the incident signals. Due to this outstanding capability, RIS is deemed a promising and revolutionary technique to enhance the coverage and the performance of wireless communication systems [1]–[4]. To

leverage these advantages, extensive research on employing RIS in communication networks has been conducted. In [5], the authors discussed the implementation of RIS in wireless networks and presented a communication-theoretic framework to analyze and design the RIS. New optimization problems have been formulated and solved in [6] to minimize the power consumption of RIS-aided communication systems by optimizing the transmit active beamforming at the source and the passive beamforming at the RIS. In [7], energy-efficient designs for both the RIS phase shifts and transmit power allocation have been developed. In [8], the fundamental capacity limit of multiple-input multiple-output (MIMO) communication systems aided by RIS has been investigated. Further work in [9] presented a detailed analysis of RIS-aided single-input single-output (SISO) communication systems. Path loss models for RIS-aided wireless systems were developed in [10]. Latency-minimization problems for RIS systems were formulated and solved for single- and multi-device scenarios in [11]. In [12] a novel two-timescale based RIS scheme has been proposed, in which the beamforming at the base station (BS) was developed based on the instantaneous channel state information (CSI) while the RIS phase shifts were designed based on long-term statistical CSI. In [13] the achievable ergodic rate of a RIS-aided MIMO communication systems was derived under Rician communication channels. In [14], an asymptotic ergodic sum rate for an RIS-aided communication systems was derived based on an infinite number of BS antennas. In [15] an ergodic rate expression of RIS-assisted MIMO systems with zero forcing (ZF) beamforming scheme was presented. Further work in [16] explored the average rate of RIS-MIMO communication systems under Rayleigh-Rician communication channels. In [17], [18] the weighted sum-rate of RIS-aided communication systems has been maximized. The design of RIS with phase shift errors has been explored in [19], [20].

Furthermore, rate splitting multiple access (RSMA) technique has been introduced and investigated in various applications to enhance the performance of multiple users multiple-input single-output (MU-MISO) communication systems [21]. RSMA scheme splits the users' messages into a common and private parts which are precoded, and superimposed in a common transmission. The users first decode the common message, then using first layer successive interference cancellation (SIC) scheme each private signal can be detected by the intended user. By tuning the power allocated to the common and private parts, RSMA can better handle the multiuser interference. Interestingly, the combination of RIS and RSMA has attracted more attention recently. In [22] the potential of synergy between RIS and RSMA has been presented, and the

A. Salem is with the Department of Electronic and Electrical Engineering, University College London, London, UK, (e-mail: a.salem@ucl.ac.uk).

K.-K. Wong is with the Department of Electronic and Electrical Engineering, University College London, London, UK, (e-mail: kai-kit.wong@ucl.ac.uk). He is also affiliated with Yonsei Frontier Lab, Yonsei University, Seoul, Korea.

C.-B. Chae is with the School of Integrated Technology, Yonsei University, Seoul, Korea, (e-mail: cbchae@yonsei.ac.kr).

Y. Zhang is with Kuang-Chi Science Limited, Hong Kong SAR, China (e-mail: yangyang.zhang@kuang-chi.com).

The work is supported by the Engineering and Physical Sciences Research Council (EPSRC) under grant EP/V052942/1 and by the National Research Foundation of Korea (NRF) Grant through the Ministry of Science and ICT (MSIT), Korea Government, under Grant 2022R1A5A1027646.

essential enhancements achieved by RIS-RSMA schemes have been identified and supported via insightful results. In [23] RIS and RSMA schemes have been implemented to assist users in dead-zone areas. A novel RIS-RSMA framework to improve MU-MISO downlink communications has been proposed in [24]. The work in [25] considered multi-RIS-assisted RSMA systems to provide ultra-reliable low latency communication with finite block-length transmission. In [26] a downlink RSMA architecture for RIS-aided multi-user communication systems has been proposed. An overview of integrating RSMA and RIS is provided in [27], where the need for integrating RSMA with RIS has been explained and a general model of a RIS-assisted RSMA system has been presented.

Most prior work in the literature designed the optimal RIS phase-shifts for narrow-band communication systems. However, it has been verified in several studies that the phase-shifts of the RIS units can vary with the frequency of incident signals. Therefore, the conventional RIS designs, that have not considered the impact of signal frequency, might not work properly in multi-band/wide-band systems. Thus the design of RIS in multi-band/wide-band networks is worth studying. The frequency-selective feature of RIS has been illustrated in some works in the literature. It has been shown that each RIS element can provide an adjustable phase-shift for messages within a specific frequency band while maintaining a nearly constant phase-shift for signals in other frequency bands [28]–[31]. In [28] a new design of the RIS in wide-band systems has been analyzed. A simpler design of the RIS with wide-band orthogonal frequency division multiplexing (OFDM) has been developed in [29]. Further work in [30] provided a tractable RIS design in multi-band systems. In [31] the authors optimized the BS-RIS association taking into account the frequency-selective characteristics of the RIS.

Accordingly, in this paper, we propose a simplified practical RIS design for a RIS-assisted multi-cell multi-band RSMA networks. More specifically, multiple BSs operate at different frequency bands and serve their associated users simultaneously with the aid of one RIS panel. To enhance the network performance, each BS is proposed to implement RSMA scheme to serve the users. Two-timescale based RIS scheme is considered. We first derive closed-form analytical expressions for the ergodic sum-rates using moment generating function (MGF) and Jensen inequality. The RIS phase shifts and the service selection of each RIS element are then designed by maximizing the ergodic sum-rates. The power allocation between the common and private parts of RSMA scheme is also considered. This is the first paper that studies RSMA scheme to overcome the frequency selectivity property of RIS. Our contributions are summarized as follows:

- 1) New two closed-form analytical expressions for the ergodic sum-rate are derived for RIS-aided multi-cell multi-band RSMA systems. The first analytical expression is derived by using MGF, while Jensen inequality is used to derive the second expression. In these derivations, ZF precoding scheme is implemented for the private messages, and maximum ratio transmission scheme (MRT) is used for the common part under Rician fading channels. The derivation of the ergodic

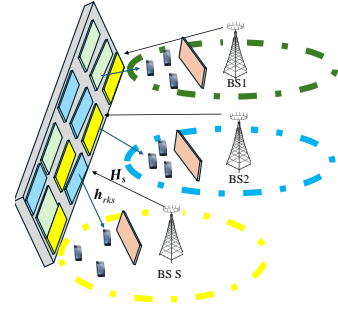


Figure 1. An RIS-aided multi-cell multi-band RSMA system.

sum-rate of RSMA scheme in RIS-aided communication systems under Rician channels is challenging and hard to consider mathematically. According to the best of our knowledge, this is the first work derives the ergodic sum rate of RSMA scheme in RIS-aided multi-cell multi-band networks. The obtained sum-rate formulas are explicit and offer numerous significant practical design insights.

- 2) Based on the analytical sum-rate expressions, practical RIS design is obtained by maximizing the achievable sum-rate subject to practical RIS reflections, quality of services (QoS) and RSMA constraints. To solve this challenging problem, fractional programming (FP) method is used to transform the logarithmic and fractional objective function into a more tractable form. The block coordinate descent (BCD) method is then employed to decouple the original problem into sub-problems. Subsequently, efficient algorithms based on the alternating direction method of multipliers (ADMM) are developed to solve these sub-problems. A power allocation scheme to split the total transmit power between the common and private parts is also considered to maximize the resulting sum-rate.
- 3) Sub-optimal designs based on the derived expressions and QoS are also presented and discussed. In the first design, we obtain the optimal RIS design that satisfies QoS of all users. In the second we consider time division (TD) protocol, in which all the RIS elements serve only one BS in different time slots. In the third design, RIS elements division (ED) protocol is studied, where the RIS elements are divided into tiles, and each tile is assigned to a BS.
- 4) Numerical and simulation results are presented to confirm the analysis and show the effectiveness of the proposed algorithms and confirm the substantial performance enhancement achieved by the proposed RIS design in multi-cell multi-band communication networks.

II. SYSTEM MODEL

We consider a RIS-aided multi-cell multi-band RSMA network as depicted in Fig. 1, where one RIS consists of M reflecting elements is implemented to assist the downlink transmissions for S BSs operating at different frequency bands. More specific, the s^{th} BS is equipped with N_s antennas

and sends independent data to K_s single-antenna users at frequency f_s using RSMA technique. The channels from the s^{th} BS to the RIS is $\mathbf{H}_s \in M \times N_s$, and from the RIS to the k_s -th user is $\mathbf{h}_{r,k_s} \in M$. Considering the RIS is often installed on tall buildings and placed close to the users, \mathbf{H}_s is modeled as a Rician fading channel, while \mathbf{h}_{r,k_s} has high line-of-sight (LoS) probability [12], [32]–[34]. For analytical tractability, we can write

$$\mathbf{H}_s = l_s \left(\sqrt{\frac{\kappa_s}{\kappa_s + 1}} \tilde{\mathbf{H}}_s + \sqrt{\frac{1}{\kappa_s + 1}} \tilde{\mathbf{H}}_s \right), \quad (1)$$

where l_s is the path-loss factor, κ_s is the Rician factor, $\tilde{\mathbf{H}}_s$ and $\tilde{\mathbf{H}}_s$ are the non-LoS (NLOS) and LoS components. The LoS components $\tilde{\mathbf{H}}_s$ and $\tilde{\mathbf{h}}_{r,k_s}$ can be expressed as

$$\tilde{\mathbf{H}}_s = \mathbf{a}_N(\phi_r^a, \phi_r^e) \mathbf{a}_M^H(\phi_t^a, \phi_t^e), \quad \tilde{\mathbf{h}}_{r,k_s} = l_{k_s} \mathbf{a}_M(\phi_{ir}^a, \phi_{ir}^e) \quad (2)$$

where l_{k_s} is the path-loss factor, ϕ_{ir}^a, ϕ_{ir}^e are the RIS-user i azimuth and elevation angles of arrival, $\phi_t^a, \phi_t^e, \phi_r^a, \phi_r^e$ denote the BS-RIS azimuth and elevation angles of departure and arrivals respectively.

A. RIS Reflection Model

Recent works illustrate that each RIS reflecting element can be adjusted to serve a certain BS that operates with a certain frequency with a tunable ideal phase-shift (i.e., $0 \sim 2\pi$), while serving the other BSs that operate with different frequency bands with almost fixed phase-shift (0 or 2π) [28]–[31]. This frequency-selective characteristic motivates us to consider the practical RIS design using the ideal phase-shifts and a binary frequency indicator, which can simplify the practical RIS model and reduce the complexity of RIS design [30], [31].

Accordingly, we can define the service selection vector for the m -th reflecting element as $\mathbf{v}_m = [v_{1,m}, \dots, v_{s,m}]^T$, where $v_{s,m} \in \{0, 1\}$, $v_{s,m} = 1$ represents that m -th element serves the s -th BS with a fully tunable phase-shift ($0 \sim 2\pi$) response, and $v_{s,m} = 0$ indicates that the m -th reflecting element provides a fixed (0 or 2π) phase-shift for the s^{th} BS. Thus each reflecting element can serve only one BS, and this can be represented of element m as $\|\mathbf{v}_m\|_0 \leq 1$, $v_{s,m} \in \{0, 1\}, \forall s, m$. Accordingly, the service selection matrix for the RIS can be defined as $\mathbf{V} = [\mathbf{v}_1, \dots, \mathbf{v}_M] \in S \times M$. The s^{th} row in \mathbf{V} represents the service selection vector for the s^{th} BS, $\tilde{\mathbf{v}}_s = [v_{s,1}, \dots, v_{s,M}]^T$. Thus, the service selection matrix for the RIS can also be expressed as $\mathbf{V} = [\tilde{\mathbf{v}}_1, \dots, \tilde{\mathbf{v}}_S]^T$. In addition, the ideal phase-shift vector for the s^{th} BS is $\phi_s = [\phi_{s,1}, \dots, \phi_{s,M}]^T$, $\phi_{s,m} \in (0, 2\pi]$. Finally, combining both the service selection and the ideal phase shift, we can introduce the practical RIS reflection model of the s^{th} BS as $\theta_s = e^{j\phi_s \odot \tilde{\mathbf{v}}_s}, \forall s$, $\phi_{s,m} \in (0, 2]$, $\|\mathbf{v}_m\|_0 \leq 1$, $v_{s,m} \in \{0, 1\}, \forall s, m$, and the reflecting coefficient matrix of the RIS as $\Theta_s = \text{diag}\{\theta_s\}$ where $\theta_s = [\theta_{s,1}, \dots, \theta_{s,M}]^T$.

B. Rate Splitting Signal Model

By implementing RSMA scheme, each BS splits each message into private and common parts. For the s^{th} BS the signal

of the k_s^{th} user is split into common part, x_{s,c,k_s} and private part, x_{s,k_s} . The common parts of all users will be packed to form the common message, $x_{s,c} = \{x_{s,c_1}, \dots, x_{s,c_{K_s}}\}$. The resulting $K_s + 1$ symbols can be presented as $\mathbf{x}_s = [x_{s,c}, x_{s,1}, \dots, x_{s,K_s}]^T \in \mathbb{C}^{K_s+1}$, where $\mathcal{E}\{\mathbf{x}_s \mathbf{x}_s^H\} = \mathbf{I}$. The symbols are then precoded via a precoding matrix defined by $\mathbf{W}_s = [\mathbf{w}_{s,c}, \mathbf{w}_{s,1}, \dots, \mathbf{w}_{s,K_s}]$ where $\mathbf{w}_{s,c} \in \mathbb{C}^{N_s}$ is the common precoder vector and $\mathbf{w}_{s,k_s} \in \mathbb{C}^{N_s}$ is the k_s^{th} private precoder vector. Accordingly, the transmitted signal by the s^{th} BS is given by [21]

$$\mathbf{s}_s = \mathbf{W}_s \mathbf{x}_s = \sqrt{P_{s,c}} \mathbf{w}_{s,c} x_{s,c} + \sum_{i=1}^{K_s} \sqrt{P_{s,p}} \mathbf{w}_{s,i} x_{s,i}, \quad (3)$$

where $P_{s,c} = (1 - t_s) P_s$ is the power allocated to the common message at the s^{th} BS with $0 < t_s \leq 1$ and P_s is the total power, while $P_{s,p} = \frac{t_s P_s}{K_s}$ is the power allocated to the private message at the s^{th} BS. The received signal at the k_s -th user can be expressed as

$$y_{s,k_s} = \sqrt{P_{s,c}} \mathbf{g}_{k_s} \mathbf{w}_{s,c} x_{s,c} + \mathbf{g}_{k_s} \sum_{i=1}^{K_s} \sqrt{P_{s,p}} \mathbf{w}_{s,i} x_{s,i} + n_{k_s}, \quad (4)$$

where $\mathbf{g}_{k_s} = \mathbf{h}_{r,k_s}^H \Theta_s \mathbf{H}_s$, $n_{k_s} \sim \mathcal{CN}(0, \sigma_{k_s}^2)$ is the additive white Gaussian noise (AWGN). At reception, each user first detects the common message and then remove it using SIC technique. Consequently, the received private message at the k_s^{th} user is given by

$$y_{s,k_s}^p = \mathbf{g}_{k_s} \sum_{i=1}^{K_s} \sqrt{P_{s,p}} \mathbf{w}_{s,i} x_{s,i} + n_{k_s}, \quad (5)$$

The signal to interference and noise ratio (SINR) of the common and private messages can be expressed as

$$\gamma_{s,k_s}^c = \frac{P_{s,c} |\mathbf{g}_{k_s} \mathbf{w}_{s,c}|^2}{P_{s,p} \sum_{i=1}^{K_s} |\mathbf{g}_{k_s} \mathbf{w}_{s,i}|^2 + \sigma_{k_s}^2}. \quad (6)$$

and

$$\gamma_{s,k_s}^p = \frac{P_{s,p} |\mathbf{g}_{k_s} \mathbf{w}_{s,k_s}|^2}{P_{s,p} \sum_{\substack{i=1 \\ i \neq k_s}}^{K_s} |\mathbf{g}_{k_s} \mathbf{w}_{s,i}|^2 + \sigma_{k_s}^2}. \quad (7)$$

The sum rate of RSMA scheme for the s^{th} BS can be calculated by

$$R_s = R_{s,c} + \sum_{k=1}^{K_s} R_{s,k}^p, \quad (8)$$

where $R_{s,c} = \min(R_{s,1}^c, \dots, R_{s,K_s}^c)$, $R_{s,k}^c$ is the common rate at the k_s^{th} user, and $R_{s,k}^p$ is the rate of the private message. The channel coding is performed over a long channel status, thus transmitting the common signal and the private signals \mathbf{s} at ergodic rates $\min_j (\mathcal{E}\{R_{s,j}^c\})_{j=1}^{K_s}$ and $\mathcal{E}\{R_{s,k}^p\}$, respectively, can guarantee successful detection at the user. Consequently, the ergodic sum rate of the s^{th} BS can be expressed as

$$\mathcal{E}\{R_s\} = \min_j (\mathcal{E}\{R_{s,j}^c\})_{j=1}^{K_s} + \sum_{k=1}^{K_s} \mathcal{E}\{R_{s,k}^p\} \quad (9)$$

The ergodic sum-rate has been analyzed in the next section using different approaches.

III. ERGODIC SUM-RATE ANALYSIS

Here we analyze the ergodic sum-rate for each BS in the network. For mathematical tractability but without loss of generality, closed form precoding techniques are implemented for the common and private messages. Precisely, the common message won't cause any interference in decoding the private signals due to use SIC. Thus, MRT precoding scheme is implemented for the common message. Also, to mitigate the inter-user interference ZF precoding technique is used for the private messages. Note that such precoding design has been adopted and validated in the literature [15], [32]. Thus, the MRT and the ZF precoders can be presented, respectively, as

$$\mathbf{w}_{s,c} = \frac{\mathbf{g}_{k_s}^H}{\|\mathbf{g}_{k_s}^H\|}, \mathbf{w}_{s,k_s} = \frac{\mathbf{f}_{k_s}}{\|\mathbf{f}_{k_s}\|} \quad (10)$$

where \mathbf{f}_{k_s} is the k_s th column of the matrix $\mathbf{F}_s = \mathbf{G}_s^H (\mathbf{G}_s \mathbf{G}_s^H)^{-1}$, $\mathbf{G}_s = \mathbf{H}_{r,s}^H \Theta_s \mathbf{H}_s$, $\mathbf{H}_{r,s}^H$ is the channel matrix between the RIS and the K_s users.

A. MGF Approach

By plugging the precoding vectors in (10) into (6) the common SINR can be re-presented as

$$\gamma_{s,k_s}^c = \frac{P_{s,c} \|\mathbf{g}_{k_s}\|^2}{\frac{P_{s,p}}{[(\mathbf{G}_s \mathbf{G}_s^H)^{-1}]_{k_s, k_s}} + \sigma_{k_s}^2}. \quad (11)$$

The ergodic rate of user k_s common message is then expressed as

$$\mathcal{E} [R_{s,k_s}^c] = \mathcal{E} [\log_2 (1 + \gamma_{s,k_s}^c)]. \quad (12)$$

Lemma 1. *The ergodic rate of the common part at the k_s^{th} user associated with the s^{th} BS can be calculated by*

$$\begin{aligned} \mathcal{E} [R_{s,k_s}^c] &= \frac{1}{\ln(2)} \sum_{i=1}^n H_i \frac{1}{z_i} \left(1 - \left(1 + \frac{2\nu P_{s,c} z_i}{\sigma_{k_s}^2} \right)^{-\frac{N_s}{2}} \right) \\ &\quad \times \left(1 + \frac{P_{s,p} z_i}{\sigma_{k_s}^2 \Psi_k} \right)^{K_s - N_s - 1} \end{aligned} \quad (13)$$

where $\nu = \left(\frac{1}{1+\kappa_s} \mathbf{h}_{r,k_s}^H \mathbf{h}_{r,k_s} + \frac{\kappa_s}{1+\kappa_s} \mathbf{h}_{r,k_s}^H \Theta_s \bar{\mathbf{H}}_s^H \bar{\mathbf{H}}_s \Theta_s^H \mathbf{h}_{r,k_s} \right)$, $\Psi_k = \left[\left(\left(\frac{1}{1+\kappa_s} \right) \mathbf{H}_r^H \mathbf{H}_r + \left(\frac{\kappa_s}{1+\kappa_s} \right) \mathbf{H}_r^H \Theta_s \mathbf{a}_M^H \mathbf{a}_M \Theta_s^H \mathbf{H}_r \right)^{-1} \right]_{k_s, k_s}$, z_i and H_i are the i^{th} zero and the weighting factors, respectively, of the Laguerre polynomials tabulated in [35, (25.245)].

Proof: The proof is presented in Appendix A. ■

By substituting the private precoding vector in (10) into (7) the private SINR can be re-presented as

$$\gamma_{s,k_s}^p = \frac{P_{s,p}}{\sigma_{k_s}^2 [(\mathbf{G}_s \mathbf{G}_s^H)^{-1}]_{k_s, k_s}}. \quad (14)$$

The ergodic rate of user k_s private message is expressed as

$$\mathcal{E} [R_{s,k_s}^p] = \mathcal{E} [\log_2 (1 + \gamma_{s,k_s}^p)]. \quad (15)$$

Lemma 2. *The ergodic rate of the private message at the k_s^{th} user associated with the s^{th} BS can be calculated by*

$$\begin{aligned} \mathcal{E} [R_{s,k_s}^p] &= \sum_{i=1}^n H_i \frac{1}{y_i} \log_2 \left(1 + \frac{P_{s,p} y_i}{\sigma_{k_s}^2} \right) \\ &\quad \times \frac{(\Psi_k)^{N_s - K_s + 1} y_i^{(N_s - K)} e^{-\Psi_k y_i}}{\Gamma(N_s - K_s + 1)} dy \end{aligned} \quad (16)$$

Proof: The proof is presented in Appendix A.

Finally by substituting (13) and (16) into (9) we obtain the ergodic sum-rate. ■

B. Approximation Using Jensen inequality

A simpler ergodic sum-rate expression is derived here based on Jensen inequality. Thus, an approximation of the ergodic rate of the common message can be calculated by

$$\mathcal{E} [R_{s,k_s}^c] \approx \log_2 (1 + \mathcal{E} \{ \gamma_{s,k_s}^c \}). \quad (17)$$

Lemma 3. *The ergodic rate of the common message at the k_s^{th} user associated with the s^{th} BS can be approximated by*

$$\mathcal{E} [R_{s,k_s}^c] \approx \log_2 \left(1 + \frac{\frac{P_{s,c}}{(\kappa_s + 1)^2} \left(\kappa_s^2 a_1 + 2\kappa_s N_s M |f_k|^2 + N_s M^2 (N_s + 1) + 2\kappa_s a_2 \right)}{P_{s,p} \frac{1}{[(\mathbf{G}_s \mathbf{G}_s^H)^{-1}]_{k_s, k_s}} + \sigma_{k_s}^2} \right) \quad (18)$$

where $a_1 = \left| \bar{\mathbf{h}}_{r,k}^H \Theta_s \bar{\mathbf{H}} \bar{\mathbf{H}}^H \Theta_s^H \bar{\mathbf{h}}_{r,k} \right|^2$, $f_k = \mathbf{a}_N (\phi_r^a, \phi_r^e) \Theta_s \bar{\mathbf{h}}_{r,k}^H$, $a_2 = \bar{\mathbf{h}}_{r,k}^H \Theta_s \bar{\mathbf{H}} \bar{\mathbf{H}}^H \Theta_s \bar{\mathbf{h}}_{r,k} \bar{\mathbf{h}}_{r,k}^H \mathbf{N}_M \bar{\mathbf{h}}_{r,k}$ and $a_3 = \left(\frac{1}{1+\kappa_s} \right) \mathbf{H}_r^H \mathbf{H}_r + \left(\frac{\kappa_s}{1+\kappa_s} \right) \mathbf{H}_r^H \Theta_s \mathbf{a}_M^H \mathbf{a}_M \Theta_s^H \mathbf{H}_r$.

Proof: The proof is presented in Appendix B. ■

Now, an approximation of the ergodic rate of the private message using Jensen inequality can be calculated by

$$\mathcal{E} [R_{s,k_s}^p] \approx \log_2 \left(1 + \mathcal{E} \left\{ \frac{P_{s,p}}{\sigma_{k_s}^2 [(\mathbf{G}_s \mathbf{G}_s^H)^{-1}]_{k_s, k_s}} \right\} \right) \quad (19)$$

Lemma 4. *The ergodic rate of the private message at the k_s^{th} user associated with the s^{th} BS can be approximated by*

$$\mathcal{E} [R_{s,k_s}^p] \approx \log_2 \left(1 + \frac{P_{s,p}}{\left[\frac{1}{N_s - K_s - 1} (a_3)^{-1} \right]_{k_s, k_s} \sigma_{k_s}^2} \right) \quad (20)$$

The proof of (20) is based on the derivation in Appendix B.

C. Design Insights

The ergodic sum-rate expressions using the MGF and Jensen inequality presented in Lemmas 1-4 produce very accurate results. The accuracy of the above derivations is also confirmed by its match with simulated results in our numerical results section. These analytical expressions can be used to design the optimal system parameters and obtain the optimal performance. From the sum rate expressions, we can observe the following insights. Generally, the practical phase shifts, Θ_s , which include the ideal phase shifts, ϕ_s , and service selection matrix, \mathbf{V} , should be optimized to enhance the system performance of each BS. In addition, the performance of the RIS is highly related to the power transmission, BS antennas, and number of the RIS elements, where increasing the value of these parameters always enhances the achievable sum-rate. In case the RIS has a limited number of reflecting elements, the performance of each BS can be enhanced by increasing the transmit power and/or number of BS antennas. The RIS location has an essential impact on the system performance, as the distance to the BSs and users increases the achievable sum-rate degrades due to larger path-loss. In line with the basic principles of RSMA scheme, optimal power allocation between the common and private parts should be considered carefully. The optimal value of the power fraction for each BS, t_s , that makes RSMA outperform the conventional schemes should be obtained for each system setting. Therefore, the achievable sum-rate can be enhanced by optimizing the ideal RIS phase shifts, the service selection matrix, and the power fraction for given system settings. This will be investigated in the following Sections.

IV. SUM-RATE MAXIMIZATION PROBLEM

In this section, we aim to maximize the achievable sum-rates of the BSs by optimizing the ideal RIS phase-shifts, the service selection matrix and the power between the common and private messages, subject to QoS, RSMA and practical RIS reflection constraints. Therefore, the sum-rate maximization problem can be formulated as

$$\max_{\mathbf{V}, \Phi, t_s} \sum_{s \in S} \hat{R}_s$$

$$\text{s.t. } \theta_s = e^{j\phi_s \odot \tilde{\mathbf{v}}_s}, \forall s \quad (\text{C1})$$

$$\phi_{s,m} \in (0, 2\pi], \forall s, m \quad (\text{C2})$$

$$\|\mathbf{v}_m\|_0 \leq 1, v_{s,m} \in \{0, 1\}, \forall s, m \quad (\text{C3})$$

$$R_{s,k} \geq R_{s,k}^{th}, \forall s, k_s \quad (\text{C4})$$

$$R_{c,k_s} \geq R_{c,k_s}, \forall s, k_s, \quad (\text{C5})$$

$$0 < t_s \leq 1, \forall s \quad (\text{C6})$$

$$p_{s,c} + \sum_{k_s \in K_s} p_{s,k_s} \leq P_s, \forall s, k_s. \quad (\text{C7}) \quad (21)$$

where $R_{s,k_s}^{th} > 0$ is the minimum rate requirement of the k_s -th user served by the s -th BS. The first constraints (C1)-(C3) are for the RIS design, while (C4) illustrates that the achievable rate of the user should be larger than the threshold, which satisfies its minimum QoS requirements and guarantees the user fairness. The constraint (C5) guarantees a successful

decoding of the common message, and (C6)-(C7) to ensure that the transmit power is less than the available power budget. Addressing this non-convex problem is challenging due to the complexity of the objective function, the variables involved, and the constraints. To overcome these challenges, we employ the BCD method to decompose the original problem into various sub-problems, where the design of the optimal phase shift and service selection at the RIS and the power allocation are handled independently.

Based on (21), the ideal phase shifts and service selection matrix can be obtained by considering the following problem

$$\begin{aligned} & \max_{\Phi, \mathbf{V}} \sum_{s \in S} \hat{R}_s \\ & \text{s.t. } \theta_s = e^{j\phi_s \odot \tilde{\mathbf{v}}_s}, \forall s \\ & \phi_{s,m} \in (0, 2\pi], \forall s, m \\ & \|\mathbf{v}_m\|_0 \leq 1, v_{s,m} \in \{0, 1\}, \forall s, m \\ & R_{s,k_s} \geq R_{s,k_s}^{th}, \forall s, k_s \end{aligned} \quad (22)$$

Here, we provide a simple and very efficient method to solve this problem. To enhance the assessment of each BS proficiency in leveraging the RIS and to determine service selection. We initially assume an ideal RIS for each BS and optimal phase-shift configurations for each BS are obtained. Then, we derive the optimal service selection matrix by allocating the suitable reflecting elements to each BS.

A. Ideal Phase-shift Design

As we have explained above, here we assume the RIS is ideal for all BSs, i.e., $\tilde{\mathbf{v}}_s = \mathbf{1}, \forall s$, and ideal phase-shifts are designed for each BS. Therefore, the problem of the s^{th} BS can be reformulated as

$$\begin{aligned} & \max_{\phi_s} \sum_{k_s=1}^{K_s} R_{s,k_s}^p \\ & \text{s.t. } \phi_{s,m} \in (0, 2\pi], \forall m \\ & R_{s,k} \geq R_{s,k}^{th}, \forall k_s \end{aligned} \quad (23)$$

To obtain the ideal phase shifts, we apply the FP method to simplify the logarithmic and fractional objective function. To start with, we first represent R_{s,k_s}^p in (20) as

$$R_{s,k_s}^p = \log_2 \left(1 + \frac{(N - K - 1) P_{s,p} \theta_s^H \mathbf{B}_{k_s} \theta_s}{\theta_s^H \mathbf{A}_{k_s} \theta_s \sigma_{k_s}^2} \right) \quad (24)$$

where $\mathbf{B}_{k_s} = \frac{1}{M} \mathbf{I}_M + \delta \text{diag}(\mathbf{a}_M) \mathbf{H}_r \Lambda^{-1} \mathbf{H}_r^H \text{diag}(\mathbf{a}_M^H)$ and $\mathbf{A}_{k_s} = \left\{ \left[\Lambda^{-1} \right]_{k_s, k_s} \mathbf{B}_{k_s} - \delta \mathbf{s} \mathbf{s}^H \right\}$, $\delta = \left(\frac{\kappa_s}{1 + \kappa_s} \right)$ and $\mathbf{s} = \left[\Lambda^{-1} \mathbf{H}_r^H \text{diag}(\mathbf{a}_M^H) \right]_{(:,k)}$.

Proof: The proof is presented in Appendix C. ■

Now, we can rewrite (23) as

$$\begin{aligned} & \max_{\phi_s} \sum_{k_s=1}^{K_s} \log_2 \left(1 + \frac{(N - K - 1) P_{s,p} \theta_s^H \mathbf{B}_{k_s} \theta_s}{\theta_s^H \mathbf{A}_{k_s} \theta_s \sigma_{k_s}^2} \right) \\ & \text{s.t. } \phi_{s,m} \in (0, 2\pi], \forall m \\ & \frac{\theta_s^H \mathbf{B}_{k_s} \theta_s}{\theta_s^H \mathbf{A}_{k_s} \theta_s} \geq \Gamma_{s,k_s}^{th}, \forall k_s \end{aligned} \quad (25)$$

where $\Gamma_{s,k_s}^{th} = 2^{R_{s,k_s}^{th}} - 1$. To apply FP method, we introduce the dual variable $\alpha = [\alpha_{1,1}, \dots, \alpha_{S,K_s}]^T$, thus the problem can be equivalently written as

$$\begin{aligned} & \max_{\phi_s, \alpha} f_1 \\ & \text{s.t. } \phi_{s,m} \in (0, 2\pi], \forall m \\ & \frac{\theta_s^H \mathbf{B}_{k_s} \theta_s}{\theta_s^H \mathbf{A}_{k_s} \theta_s} \geq \Gamma_{s,k_s}^{th}, \forall k_s \end{aligned} \quad (26)$$

where $f_1 = \sum_{k_s=1}^{K_s} \log_2(1 + \alpha_{k_s}) - \sum_{k_s=1}^{K_s} \alpha_{k_s} + \sum_{k_s=1}^{K_s} \frac{(1 + \alpha_{k_s}) \theta_s^H \mathbf{B}_{k_s} \theta_s}{\theta_s^H \mathbf{C}_{k_s} \theta_s}$ and $\mathbf{C}_{k_s} = \mathbf{A}_{k_s} + \mathbf{B}_{k_s}$. For a given α , we can focus on the following problem

$$\begin{aligned} & \max_{\phi_s, \alpha} f_2 \\ & \text{s.t. } \phi_{s,m} \in (0, 2\pi], \forall m \\ & \theta_s^H \mathbf{B}_{k_s} \theta_s - \Gamma_{s,k_s}^{th} \theta_s^H \mathbf{A}_{k_s} \theta_s \geq 0, \forall k_s \end{aligned} \quad (27)$$

where $f_2 = \sum_{k_s=1}^{K_s} \frac{(1 + \alpha_{k_s}) \theta_s^H \mathbf{B}_{k_s} \theta_s}{\theta_s^H \mathbf{C}_{k_s} \theta_s}$. The frac-

tion f_2 can be also expressed as $f_2 = \sum_{k_s=1}^{K_s} (1 + \alpha_{k_s}) \theta_s^H \bar{\mathbf{B}}_{k_s} (\theta_s^H \mathbf{C}_{k_s} \theta_s)^{-1} \bar{\mathbf{B}}_{k_s} \theta_s$ where $\bar{\mathbf{B}}_{k_s} = \mathbf{B}_{k_s}^{1/2}$. The problem now is sum of ratios, thus by applying the quadratic transform in [36], [37] f_2 can be further presented as $f_3 = \sum_{k_s=1}^{K_s} 2\sqrt{(1 + \alpha_{k_s})} \text{Re} \left\{ \theta_s^H \bar{\mathbf{B}}_{k_s} \mathbf{y}_m \right\} - \sum_{k_s=1}^{K_s} \mathbf{y}_m^T (\theta_s^H \mathbf{C}_{k_s} \theta_s) \mathbf{y}_m$, where \mathbf{y}_m refers to a collection of auxiliary variables y_1, \dots, y_M . Thus, the problem can be re-formulated as

$$\begin{aligned} & \max_{\phi_s, \alpha, \mathbf{y}} \sum_{k_s=1}^{K_s} 2\sqrt{(1 + \alpha_{k_s})} \text{Re} \left\{ \theta_s^H \bar{\mathbf{B}}_{k_s} \mathbf{y}_{K_s} \right\} \\ & - \sum_{k_s=1}^{K_s} \mathbf{y}_{k_s}^T (\theta_s^H \mathbf{C}_{k_s} \theta_s) \mathbf{y}_{k_s} \\ & \text{s.t. } \phi_{s,m} \in (0, 2\pi], \forall m \\ & \theta_s^H \mathbf{B}_{k_s} \theta_s - \Gamma_{s,k_s}^{th} \theta_s^H \mathbf{A}_{k_s} \theta_s \geq 0, \forall k_s \end{aligned} \quad (28)$$

Now we can adopt the BCD method to handle the optimization variables, α , \mathbf{y}_m and ϕ_s .

Update α , and \mathbf{y}_m : with fixed \mathbf{y}_m and ϕ_s , the optimal solution of α is found to be [36], [37] $\alpha_{k_s}^* = \frac{\theta_s^H \mathbf{B}_{k_s} \theta_s}{\theta_s^H \mathbf{A}_{k_s} \theta_s}$. Similarly, the optimal solution of \mathbf{y}_m is $\mathbf{y}_m^* = (\theta_s^H \mathbf{C}_{k_s} \theta_s)^{-1} \bar{\mathbf{B}}_{k_s} \theta_s$.

Update Ideal Passive shifts θ_s : with fixed, α , \mathbf{y}_m , the problem can be reformulated as

$$\begin{aligned} & \max_{\theta_s} \sum_{k_s=1}^{K_s} 2\sqrt{(1 + \alpha_{k_s})} \text{Re} \left\{ \theta_s^H \bar{\mathbf{B}}_{k_s} \mathbf{y}_m \right\} \\ & - \mathbf{y}_m^T (\theta_s^H \mathbf{C}_{k_s} \theta_s) \mathbf{y}_m \\ & \text{s.t. } |\theta_{s,m}| = 1 \forall m \\ & \theta_s^H \mathbf{B}_{k_s} \theta_s - \Gamma_{s,k_s}^{th} \theta_s^H \mathbf{A}_{k_s} \theta_s \geq 0, \forall s, k_s \end{aligned} \quad (29)$$

The problem is still hard and difficult to solve due to the non-convexity of the unit modulus constraint. ADMM method

is employed to handle this problem, thus we introduce the auxiliary variables $\psi_s = [\psi_{s,1}, \dots, \psi_{s,M}]^T$ and reformulate the problem as

$$\begin{aligned} & \max_{\theta_s, \psi_s} \sum_{k_s=1}^{K_s} 2\sqrt{(1 + \alpha_{k_s})} \text{Re} \left\{ \theta_s^H \bar{\mathbf{B}}_{k_s} \mathbf{y}_m \right\} \\ & - \sum_{k_s=1}^{K_s} \mathbf{y}_m^T (\theta_s^H \mathbf{C}_{k_s} \theta_s) \mathbf{y}_m \\ & \text{s.t. } |\theta_{s,m}| \leq 1 \forall m \\ & |\psi_{s,m}| = 1 \forall m \\ & \theta_s = \psi_s \forall m \\ & \theta_s^H \mathbf{B}_{k_s} \theta_s - \Gamma_{s,k_s}^{th} \theta_s^H \mathbf{A}_{k_s} \theta_s \geq 0, \forall s, k_s \end{aligned} \quad (30)$$

The optimal solution can be obtained by solving the augmented Lagrangian (AL) problem. By defining the dual variables $\zeta_s = [\zeta_{s,1}, \dots, \zeta_{s,M}]^T$ and penalty coefficient $\rho > 0$, the problem can be expressed as

$$\begin{aligned} & \max_{\theta_s, \psi_s, \zeta_s} \sum_{k_s=1}^{K_s} 2\sqrt{(1 + \alpha_{k_s})} \text{Re} \left\{ \theta_s^H \bar{\mathbf{B}}_{k_s} \mathbf{y}_m \right\} \\ & - \sum_{k_s=1}^{K_s} \mathbf{y}_m^T (\theta_s^H \mathbf{C}_{k_s} \theta_s) \mathbf{y}_m \\ & - \text{Re} \left\{ \zeta_s^H (\theta_s - \psi_s) \right\} - \frac{\rho}{2} \|\theta_s - \psi_s\|_2^2 \\ & \text{s.t. } |\theta_{s,m}| \leq 1 \forall m \\ & |\psi_{s,m}| = 1 \forall m \\ & \theta_s^H \mathbf{B}_{k_s} \theta_s - \Gamma_{s,k_s}^{th} \theta_s^H \mathbf{A}_{k_s} \theta_s \geq 0, \forall s, k_s \end{aligned} \quad (31)$$

This formulation is more tractable and can be solved by updating $\theta_s, \psi_s, \zeta_s$, as follows:

Update θ_s : the problem of optimizing θ_s with fixed ψ_s, ζ_s , can be expressed as

$$\begin{aligned} & \max_{\theta_s} \sum_{k_s=1}^{K_s} 2\sqrt{(1 + \alpha_{k_s})} \text{Re} \left\{ \theta_s^H \bar{\mathbf{B}}_{k_s} \mathbf{y}_m \right\} \\ & - \sum_{k_s=1}^{K_s} \mathbf{y}_m^T (\theta_s^H \mathbf{C}_{k_s} \theta_s) \mathbf{y}_m \\ & - \text{Re} \left\{ \zeta_s^H (\theta_s - \psi_s) \right\} - \frac{\rho}{2} \|\theta_s - \psi_s\|_2^2 \\ & \text{s.t. } |\theta_{s,m}| \leq 1 \forall m \\ & \theta_s^H \mathbf{B}_{k_s} \theta_s - \Gamma_{s,k_s}^{th} \theta_s^H \mathbf{A}_{k_s} \theta_s \geq 0, \forall s, k_s \end{aligned} \quad (32)$$

This problem is convex and thus can be easily solved using software tools as CVX.

Update ψ_s : the problem of optimizing ψ_s with fixed θ_s, ζ_s , can be written as

$$\begin{aligned} & \max_{\psi} - \sum_{k_s=1}^{K_s} \text{Re} \left\{ \zeta_s^H (\theta_s - \psi_s) \right\} - \frac{\rho}{2} \|\theta_s - \psi_s\|_2^2 \\ & \text{s.t. } |\psi_{s,m}| = 1 \forall m \end{aligned} \quad (33)$$

which can be written as

Algorithm 1 ADMM based ideal RIS phase-shifts design algorithm.

1. Initialize ψ_s, ζ_s .
2. Repeat
3. Calculate passive beamforming θ_s from (32);
4. Calculate auxiliary variable ψ_s using (36);
5. Update Lagrangian multiplier ζ_s by (37);
6. until convergence.

$$\begin{aligned} \max_{\psi} - \sum_{k_s=1}^{K_s} \mathbf{Re} \left\{ (\zeta_s + \rho \theta_s)^H \psi_s \right\} - \frac{\rho}{2} \|\theta_s\|_2^2 \\ - \frac{\rho}{2} \|\theta_s\|_2^2 - \mathbf{Re} \{ \zeta_s \theta_s \} \\ \text{s.t. } |\psi_{s,m}| = 1 \forall m \end{aligned} \quad (34)$$

where $\|\theta_s\|_2^2 = M$. Thus, the problem can be further reduced to

$$\begin{aligned} \max_{\psi_s} \sum_{k_s=1}^{K_s} \mathbf{Re} \left\{ (\zeta_s + \rho \theta_{k_s})^H \psi_{k_s} \right\} \\ \text{s.t. } |\psi_{s,m}| = 1 \forall m \end{aligned} \quad (35)$$

The optimal solution can be obtained as [28]–[31]

$$\psi_s^* = e^{j\angle(\zeta_s + \rho \theta_s)^H}. \quad (36)$$

Update ζ_s : we can update the dual variable ζ_s by [28]–[31]

$$\zeta_s = \zeta_s + \rho(\theta_s - \psi_s). \quad (37)$$

Finally, the ADMM-based ideal RIS phase-shift design is summarized in Algorithm 1.

B. Service Selection Design

Now with obtaining the ideal phase shifts, the optimization problem to obtain the service selection matrix \mathbf{A} can be formulated as

$$\begin{aligned} \max_{\mathbf{V}} \sum_{s \in S} \sum_{k_s=1}^{K_s} \log_2 \left(1 + \frac{(N-K-1) P_{s,p} \theta_s^H \mathbf{B}_{k_s} \theta_s}{\theta_s^H \mathbf{A}_{k_s} \theta_s \sigma_{k_s}^2} \right) \\ \text{s.t. } \theta_s = e^{j\phi_s \odot \tilde{\mathbf{v}}_s}, \forall S \\ \|\mathbf{v}_m\|_0 \leq 1, v_{s,m} \in \{0, 1\}, \forall s, m \\ \frac{\theta_s^H \mathbf{B}_{k_s} \theta_s}{\theta_s^H \mathbf{A}_{k_s} \theta_s} \geq \Gamma_{s,k_s}^{th}, \forall s, k_s \end{aligned} \quad (38)$$

which can be equivalently expressed as

$$\begin{aligned} \max_{\mathbf{V}} \sum_{s \in S} \sum_{k_s=1}^{K_s} \log_2 \left(1 + \frac{\mathbf{b}_1 \mathbf{B}_{k_s} \mathbf{b}_1^T}{\mathbf{b}_1 \mathbf{A}_{k_s} \mathbf{b}_1^T} \right) \\ \text{s.t. } \theta_s = e^{j\phi_s \odot \tilde{\mathbf{v}}_s}, \forall S \\ \|\mathbf{v}_m\|_0 \leq 1, v_{s,m} \in \{0, 1\}, \forall s, m \\ \frac{\mathbf{b}_1 \mathbf{B}_{k_s} \mathbf{b}_1^T}{\mathbf{b}_1 \mathbf{A}_{k_s} \mathbf{b}_1^T} \geq \Gamma_{s,k_s}^{th}, \forall s, k_s \end{aligned} \quad (39)$$

where $\mathbf{b}_1 = \left(\tilde{\mathbf{v}}_s^H (\text{diag} \{ e^{j\phi_s^H} \} - \mathbf{I}_M) + \mathbf{1} \right)$.

Proof: The SINR can be reformulated as

$$\frac{\theta_s^H \mathbf{B}_{k_s} \theta_s}{\theta_s^H \mathbf{A}_{k_s} \theta_s} =$$

$$\begin{aligned} & \frac{\left(\tilde{\mathbf{v}}_s^H \odot e^{j\phi_s^H} + (1 - \tilde{\mathbf{v}}_s^H) \right) \mathbf{B}_{k_s} \left(\tilde{\mathbf{v}}_s \odot e^{j\phi_s} + (1 - \tilde{\mathbf{v}}_s) \right)}{\left(\tilde{\mathbf{v}}_s^H \odot e^{j\phi_s^H} + (1 - \tilde{\mathbf{v}}_s^H) \right) \mathbf{A}_{k_s} \left(\tilde{\mathbf{v}}_s \odot e^{j\phi_s} + (1 - \tilde{\mathbf{v}}_s) \right)} = \\ & \frac{\left(\tilde{\mathbf{v}}_s^H \text{diag} \{ e^{j\phi_s^H} \} + (1 - \tilde{\mathbf{v}}_s^H) \right) \mathbf{B}_{k_s} \left(\text{diag} \{ e^{j\phi_s} \} \tilde{\mathbf{v}}_s + (1 - \tilde{\mathbf{v}}_s) \right)}{\left(\tilde{\mathbf{v}}_s^H \text{diag} \{ e^{j\phi_s^H} \} + (1 - \tilde{\mathbf{v}}_s^H) \right) \mathbf{A}_{k_s} \left(\text{diag} \{ e^{j\phi_s} \} \tilde{\mathbf{v}}_s + (1 - \tilde{\mathbf{v}}_s) \right)} = \\ & \frac{\left(\tilde{\mathbf{v}}_s^H \left(\text{diag} \{ e^{j\phi_s^H} \} - \mathbf{I}_M \right) + \mathbf{1} \right) \mathbf{B}_{k_s} \left(\left(\text{diag} \{ e^{j\phi_s} \} - \mathbf{I}_M \right) \tilde{\mathbf{v}}_s + \mathbf{1} \right)}{\left(\tilde{\mathbf{v}}_s^H \left(\text{diag} \{ e^{j\phi_s^H} \} - \mathbf{I}_M \right) + \mathbf{1} \right) \mathbf{A}_{k_s} \left(\left(\text{diag} \{ e^{j\phi_s} \} - \mathbf{I}_M \right) \tilde{\mathbf{v}}_s + \mathbf{1} \right)} = \\ & \frac{\mathbf{b}_1 \mathbf{B}_{k_s} \mathbf{b}_1^T}{\mathbf{b}_1 \mathbf{A}_{k_s} \mathbf{b}_1^T}. \end{aligned} \quad (40)$$

FP is applied to simplify the problem tractability. To apply FP method, we first define the dual variable $\alpha = [\alpha_{1,1}, \dots, \alpha_{S,K_s}]^T$, thus the problem can be written as

$$\begin{aligned} \max_{\mathbf{V}, \alpha} f_1 \\ \text{s.t. } \theta_s = e^{j\phi_s \odot \tilde{\mathbf{v}}_s}, \forall S \\ \|\mathbf{v}_m\|_0 \leq 1, v_{s,m} \in \{0, 1\}, \forall s, m \\ \frac{\mathbf{b}_1 \mathbf{B}_{k_s} \mathbf{b}_1^T}{\mathbf{b}_1 \mathbf{A}_{k_s} \mathbf{b}_1^T} \geq \Gamma_{s,k_s}^{th}, \forall s, k_s \end{aligned} \quad (41)$$

where $f_1 = \sum_{s \in S} \sum_{k_s=1}^{K_s} \log_2(1 + \alpha_{k_s}) - \sum_{s \in S} \sum_{k_s=1}^{K_s} \alpha_{k_s} + \sum_{s \in S} \sum_{k_s=1}^{K_s} \frac{(1 + \alpha_{k_s}) \mathbf{b}_1 \mathbf{B}_{k_s} \mathbf{b}_1^T}{\mathbf{b}_1 \mathbf{C}_{k_s} \mathbf{b}_1^T}$ and $\mathbf{C}_{k_s} = \mathbf{A}_{k_s} + \mathbf{B}_{k_s}$. Similarly, with fixed θ_s , the optimal $\alpha_{k_s}^* = \frac{\mathbf{b}_1 \mathbf{B}_{k_s} \mathbf{b}_1^T}{\mathbf{b}_1 \mathbf{A}_{k_s} \mathbf{b}_1^T}$. For a given α_{k_s} , by applying the quadratic transform in [36], [37] the problem can be presented as

$$\begin{aligned} \max_{\mathbf{V}} f_2 \\ \text{s.t. } \theta_s = e^{j\phi_s \odot \tilde{\mathbf{v}}_s}, \forall S \\ \|\mathbf{v}_m\|_0 \leq 1, v_{s,m} \in \{0, 1\}, \forall s, m \\ \frac{\mathbf{b}_1 \mathbf{B}_{k_s} \mathbf{b}_1^T}{\mathbf{b}_1 \mathbf{A}_{k_s} \mathbf{b}_1^T} \geq \Gamma_{s,k_s}^{th}, \forall s, k_s \end{aligned} \quad (42)$$

where $f_2 = \sum_{s \in S} \sum_{k_s=1}^{K_s} \frac{(1 + \alpha_{k_s}) \mathbf{b}_1 \mathbf{B}_{k_s} \mathbf{b}_1^T}{\mathbf{b}_1 \mathbf{C}_{k_s} \mathbf{b}_1^T}$, which can be simplified to, $f_3 = \sum_{s \in S} \sum_{k_s=1}^{K_s} 2\sqrt{(1 + \alpha_{k_s})} \mathbf{Re} \{ \mathbf{y}_m^T \bar{\mathbf{B}}_{k_s} \mathbf{b}_1^T \} - \sum_{k_s=1}^{K_s} \mathbf{y}_m^T \mathbf{b}_1 \mathbf{C}_{k_s} \mathbf{b}_1^T \mathbf{y}_m$ [36], [37]. Thus, we can write the problem as

$$\begin{aligned} \max_{\mathbf{V}, \mathbf{y}} f_3 \\ \text{s.t. } \theta_s = e^{j\phi_s \odot \tilde{\mathbf{v}}_s}, \forall S \\ \|\mathbf{v}_m\|_0 \leq 1, v_{s,m} \in \{0, 1\}, \forall s, m \\ \mathbf{b}_1 \mathbf{B}_{k_s} \mathbf{b}_1^T \geq \Gamma_{s,k_s}^{th} \mathbf{b}_1 \mathbf{A}_{k_s} \mathbf{b}_1^T \forall s, k_s \end{aligned} \quad (43)$$

With fixed \mathbf{V} the optimal solution of \mathbf{y} is found to be [36], [37] $\mathbf{y}_m^* = \left(\theta_s^H \mathbf{C}_{k_s} \theta_s \right)^{-1} \bar{\mathbf{B}}_{k_s} \theta_s$. Each element of \mathbf{V}

is binary, $v_{s,m} \in \{0, 1\}$, the 0-norm constraint, $\|\mathbf{v}_m\|_0$, can be equivalently transformed into, $\|\mathbf{v}_m\|_0 = \|\mathbf{v}_m\|_1 = \mathbf{1}^T \mathbf{v}_m \leq 1$. Then, invoking the difference-of-convex function method, the constraint $v_{s,m} \in \{0, 1\}$ can be transformed into $0 \leq v_{s,m} \leq 1$ and $\sum_{s \in S} (\mathbf{1}^T \mathbf{v}_m - \mathbf{v}_m^T \mathbf{v}_m) \leq 0$. We further apply the penalty and reformulate the problem as

$$\begin{aligned} & \max_{\mathbf{V}} f_4 \\ \text{s.t.} \quad & \mathbf{1}^T \mathbf{v}_m \leq 1 \forall m \\ & 0 \leq v_{s,m} \leq 1, \forall s, m \\ & \mathbf{b}_1 \mathbf{B}_{k_s} \mathbf{b}_1^T \geq \Gamma_{s,k_s}^{th} \mathbf{b}_1 \mathbf{A}_{k_s} \mathbf{b}_1^T \forall s \end{aligned} \quad (44)$$

where $f_4 = \sum_{s \in S} \sum_{k_s=1}^{K_s} 2\sqrt{(1 + \alpha_{k_s})} \text{Re} \{ \mathbf{y}_m^T \bar{\mathbf{B}}_{k_s} \mathbf{b}_1^T \} - \sum_{k_s=1}^{K_s} \mathbf{y}_m^T (\mathbf{b}_1 \mathbf{C}_{k_s} \mathbf{b}_1^T) \mathbf{y}_m - \tau \sum_{s \in S} (\mathbf{1}^T \tilde{\mathbf{v}}_s - \tilde{\mathbf{v}}_s^T \tilde{\mathbf{v}}_s)$ and $\tau > 0$ is a penalty factor. By utilizing the first-order Taylor expansion, the problem can be solved using software tools as CVX.

C. Sub-optimal Design

In this sub-section, we provide some sub-optimal designs of an RIS assisted multi-cell multi-band communication systems.

1) *QoS design*: Unlike the iterative solutions, here, we obtain the service selection matrix \mathbf{V} theoretically using the derived ergodic sum rate expressions. Since the service selection matrix \mathbf{V} is directly affect the users QoS, we obtain \mathbf{V} that satisfies QoS constraint of all users, i.e., $\mathbf{b}_1 \mathbf{B}_{k_s} \mathbf{b}_1^T \geq \Gamma_{s,k_s}^{th} \mathbf{b}_1 \mathbf{A}_{k_s} \mathbf{b}_1^T, \forall s, k_s$. Thus, for user k_s served by BS S , we can get $\frac{\mathbf{b}_1 \mathbf{B}_{k_s} \mathbf{b}_1^T}{\mathbf{b}_1 \mathbf{A}_{k_s} \mathbf{b}_1^T} = \Gamma_{s,k_s}^{th}$. Let us express the two terms explicitly, the ratio simplifies to

$$\sum_{i,j} B_{i,j} b_i^T b_j - \Gamma_{s,k_s}^{th} \sum_{i,j} A_{i,j} b_i^T b_j = 0 \quad (45)$$

where $A_{i,j}$, $B_{i,j}$ and b_j are the elements of \mathbf{A}_{k_s} , \mathbf{B}_{k_s} and \mathbf{b}_1 , respectively. We can find \tilde{v}_i using simple linear search algorithm, by activating the elements until the condition in (45) satisfied, e.g., search through all possible binary vector to find the solution that satisfies (45).

2) *Time division (TD) protocol*: In this design, all the RIS elements serve only one BS in different time slots. In each time slot, one BS transmits messages to the users via the RIS, where the entire RIS is configured for the active BS. Thus number of time slots, T , is identical to number of BSs. The achievable sum-rate for each BS in TD design can be evaluated by, $R_s^{TD} = \frac{1}{S} R_s$. The optimal phase shifts of the RIS at each time slot for each BS can be obtained by using the solution in Section IV-A.

3) *RIS elements division (ED) protocol*: In this design, the RIS elements are divided equally into tiles, and each tile is assigned to a BS. Number of elements assigned for each BS, the tile size, is $\frac{M}{S}$. The optimal phase shifts of each tile can be obtained by using the solution in Section IV-A.

Algorithm 2 GS method.

- 1: Initialize $\varrho = 0$, $\lambda = 1$, and $\zeta = \frac{-1+\sqrt{5}}{2}$.
 - 2: Repeat
 - 3: Update $t_{s1} = \varrho + (1 - \zeta)\lambda$ and $t_{s2} = \lambda + (1 - \zeta)\varrho$.
 - 4: Obtain $R(t_{s1})$ and $R(t_{s2})$ from (9).
 - 5: If $R(t_{s1}) > R(t_{s2})$, set $\varrho = t_{s1}$. Else set $\zeta = t_{s2}$.
 - 6: Until $|\varrho - \lambda|$ converges.
 - 7: Find $ts^* = (\varrho + \lambda)/2$.
-

Algorithm 3 Practical RIS Design and RSMA power allocation for sum-rate maximization problem.

- 1: Initialize \mathbf{V} , ψ_s , ζ_s , α , \mathbf{y} and θ_s ;
 - 2: for $s = 1$ to S do;
 - 4: Calculate dual and auxiliary variables;
 - 5: Update ideal phase-shifts by Algorithm 1;
 - 6: end for;
 - 6: Obtain \mathbf{V} by solving (44);
 - 7: Repeat until convergence.
 - 8: Allocate the power by Algorithm 2.
 - 9: Return ϕ , \mathbf{V} , and t_s .
-

D. RSMA Power Allocation

The optimal power fraction for each BS, t_s , can be calculated by solving the following maximization problem

$$\max_{0 \leq t_s \leq 1} \left(\min_j (\mathcal{E} \{ R_{s,j}^c \})_{j=1}^{K_s} + \sum_{k=1}^{K_s} \mathcal{E} \{ R_{s,k}^p \} \right) \quad (46)$$

The optimal value of t_s can be determined using the first-order (derivative) condition. However, given the ergodic rate expressions, the solution would be complicated. A basic one-dimensional search methods such as golden section (GS) technique over the period $0 \leq t_s \leq 1$ can be applied to obtain the optimal power fraction t_s . GS algorithm to reach the optimal t_s is presented in Algorithm 2.

To reduce the complexity, an effective power allocation scheme has been proposed in [38]. Basically, a part (t_s) of the total power is allocated to the private signals to perform approximately the same sum rate as that achieved by the conventional multiple-user transmission, NoRS, with full power. Then, the rest of the total power can be allocated to the common message [38]. The sum-rate gain of RSMA over NoRS can be evaluated by $\Delta R_s = \mathcal{E} \{ R_{s,c} \} + \sum_{k=1}^{K_s} (\mathcal{E} \{ R_{s,k}^p \} - \mathcal{E} \{ R_k^{NoRS} \})$. Thus, the optimal ratio, t_s , can be obtained by achieving the equality, $\mathcal{E} \{ R_{s,k}^p \} \approx \mathcal{E} \{ R_k^{NoRS} \}$.

Finally, according to the above analysis, the total steps to obtain the optimal practical RIS design and RSMA power allocation are summarized in Algorithm 3.

V. NUMERICAL RESULTS

In this section, simulation and numerical results are presented to confirm the accuracy of the derived analytical expressions and demonstrate the effectiveness of the proposed

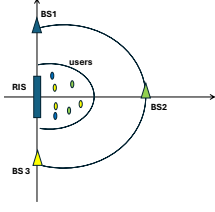


Figure 2. An illustration of the RIS, BSs, and users locations.

algorithms. It is assumed that the multi-cell system consists of $S = 3$ BSs/cells, and the users experience similar noise variance, σ^2 , thus the transmit SNR at each BS is $\gamma = \frac{P_s}{\sigma^2}$. The QoS requirement of each user is $\Gamma_{s,k_s}^{th} = 5$ dB $\forall s, k_s$. A two-dimensional coordinate system is considered where the RIS is situated at $(0, 0)$, and the BSs are located 50 m away from the RIS. In addition, the users in each cell are located 2 m away from the RIS as shown in Fig. 2.

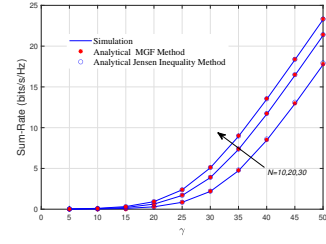
A. Ergodic sum-rate analysis

Firstly, to validate the ergodic sum-rates expressions derived in this work based on MGF and Jensen inequality methods, in Fig. 3, we plot the ergodic sum-rate with respect to the transmit SNR, γ . Fig. 3a, presents the ergodic sum-rate for different numbers of BS antennas, $N_s = 10, 20$ and 30, and number of RIS elements is $M = 5$, while Fig. 3b, shows the ergodic sum-rate with when $N_s = 30$, and $M = 5$ and 10. In these figures, the simulation results are presented by solid lines, while the analytical results based on MGF and Jensen inequality approaches are presented by star and circle markers, respectively. It is evident that the simulation and analytical results are in good agreement, thereby validating the derivations presented in Section (III). It is also apparent that the achievable sum-rate enhances with increasing the transmit SNR. From Figs. 3a and 3b, it can be noted that using large number of BS antennas N_s and RIS elements M leads to improve the achievable sum-rate.

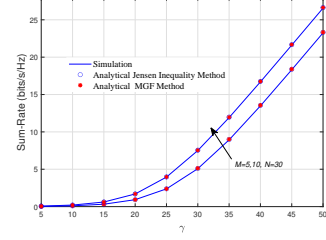
Furthermore, in Fig. 4, we illustrate the ergodic sum-rate of the RSMA and NoRS schemes versus transmit SNR for different numbers of users, $K_s = 2$ and 3, when $N_s = 15$, $M = 5$ and the distances are normalized. The results in this figure explain clearly the benefits of using RSMA over the conventional NoRS schemes, and justify the implementation of RSMA in such RIS communication systems. RSMA scheme outperforms the conventional NoRS technique with almost an up to 5dB gain in the SNR for a given sum rate. In addition, as expected increasing number of users always enhances the achievable sum-rates for both schemes.

B. Ideal RIS design

Fig. 5 plots the achievable sum-rates with both optimal and random phase shifts when $N_s = 30$ and $M = 10$. It can be observed that the ergodic sum-rate utilizing the optimal phase shifts is much higher than the ergodic sum-rate utilizing random phase shifts. Thus, the optimal phase shifts result in significant SNR gains compared to the random phase shifts.



(a) Sum-rate versus transmit SNR for different number of BSs antennas when $M = 5$.



(b) Sum-rate versus transmit SNR for different number of RIS elements when $N_s = 30$.

Figure 3. Sum-rate versus transmit SNR for different numbers of BS antennas and RIS elements.

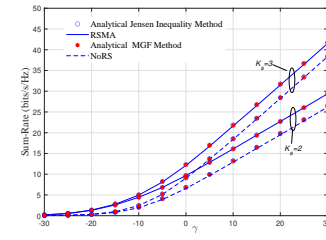


Figure 4. Sum-rate versus transmit SNR with different numbers of users K_s for RSMA and NoRS schemes.

The gain attained using the optimal phase shifts over the random phase shifts is about 12dB for a given sum-rate value.

In addition, Fig. 6 illustrates the achievable users rates for different QoS requirements, Γ_{s,k_s} , when $N_s = 10$, and $M = 5$. Firstly, in Fig. 6a we present the users rates when the QoS requirement of each user is relatively low and achievable. In this case, to maximize the sum-rate, the RIS phase shifts have been designed to reflect most of the beam toward the best user's channel which is in this case user 1, while the other two users achieve almost similar rates. Then, in Fig. 6b we increase the QoS requirement of the weak user, user 3. As we can see, in this case, the RIS is designed to provide more power toward

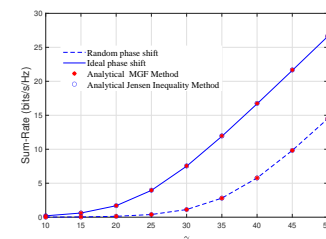


Figure 5. Ergodic sum-rates versus transmit SNR, γ , for different phase shifts.

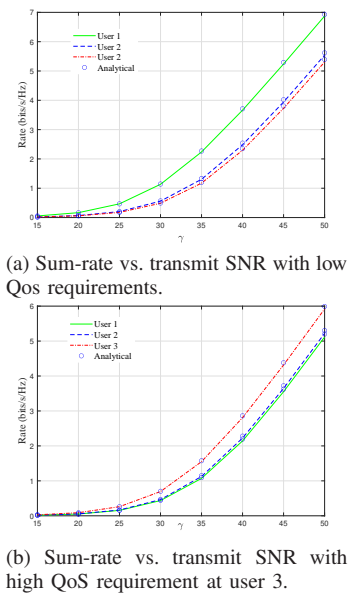


Figure 6. Sum-rate vs. transmit SNR for different QoS requirements.

user 3 and thus enhance the achievable rate at user 3 on the expenses of user 1 performance and the achievable sum-rate. It is evident from these results that the QoS constraints should be adjusted to provide fairness between the users.

C. Practical RIS design

Fig. 7 shows the total sum-rates versus the transmit SNR for two scenarios $S = 2$ and $S = 3$ when $M = 10$, $N_s = 30$, and $K = 3$. Fig. 7a shows the case when $S = 2$ and Fig. 7b shows the case $S = 3$. Additionally, to provide fair comparisons, results of ED and TD protocols are added as benchmarks. It can be seen that the proposed algorithm has greater performance than the other schemes under different settings. The proposed algorithm provides up to 3dB gain when $S = 2$ and 5dB gain when $S = 3$ compared with the ED protocol and 10 dB gain when $S = 2$ and 15 dB gain when $S = 3$ compared with the TD protocol.

To consider the effect of the RIS location on the system performance, we illustrate the total sum-rate versus the BS-RIS distance in Fig. 8 (a) and versus the RIS-user distance in Fig. 8 (b). It can be observed that when the RIS is located far away from the BS and/or the users, the achievable sum-rates deteriorate. This is because the reflected signals from the RIS become weaker due to larger path-loss. Having said that, the sum-rate is more sensitive to the RIS-user distance than BS-RIS distance, as we can notice the sum-rate degrades fast as the users move away from the RIS. Increasing the transmit power, number of BS antennas and/or RIS elements can tackle this issue. Our proposed algorithm always performs better than the other schemes under different RIS and users' locations.

To illustrate the convergence of the proposed algorithm, the total sum-rate versus the number of iterations is plotted in Fig. 9 when $N_s = 30$, $M = 10$, $\gamma = 40$ dB for $S = 2$ and 3. As we can see, the convergence is reached after a limited number of iterations under different system parameters.

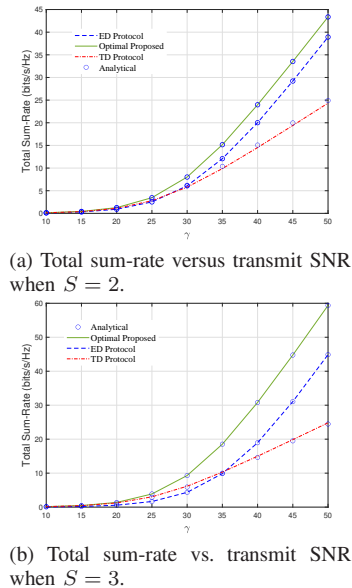


Figure 7. Total sum-rate vs. transmit SNR for different number of BSs.

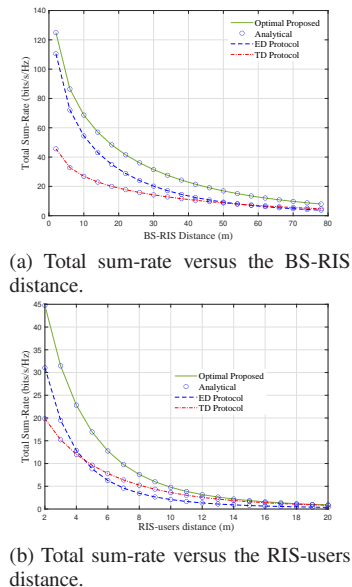


Figure 8. Total sum-rate vs. the BS-RIS distance, and RIS-users distance when $\gamma = 45$ dB.

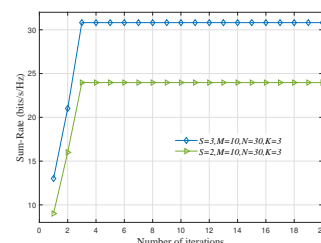


Figure 9. Convergence of the proposed algorithm.

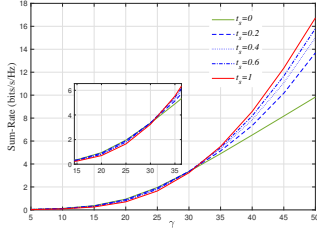


Figure 10. Sum-rate vs. transmit SNR for various values of t_s .

D. RSMA Power Allocation

In Fig. 10, we plot the achievable sum-rate versus transmit SNR for different values of t_s , when $N_s = 30$, $M = 10$, and $K = 3$. Interestingly enough, it can be observed that at low and medium SNR values, $\text{SNR} \leq 32$ dB, the optimal value of t_s in these ranges is approximately close to 0. This means, in this case, most of the power should be allocated to the common part. However, at high SNR values, $\text{SNR} \geq 32$ dB, the achievable sum-rate enhances as the power fraction t_s increases. Thus, in this SNR range, most of the power should be allocated to the private part.

VI. CONCLUSION

In this work, we first provided two methods to derive the ergodic sum-rate for RIS-assisted multi-cell multi-band RSMA communication systems. Then based on the analytical derivation, we investigated the RIS reflection design and RSMA power allocation scheme for the total sum-rate maximization problem. Efficient algorithms have been proposed to solve the total sum-rate optimization problem by exploiting BCD, ADMM, and line search algorithms. Numerical results showed that significant performance improvement can be attained using the proposed algorithms, which converge after a few iterations. Additionally, the users' performance can be controlled by adjusting the phase shifts according to their QoS requirements.

APPENDIX A

For any $u, v > 0$, the ergodic rate can be calculated using the MGFs by [39]

$$\mathcal{E} \left[\ln \left(1 + \frac{u}{v} \right) \right] = \int_0^\infty \frac{1}{z} (\mathcal{M}_v(z) - \mathcal{M}_{u,v}(z)) dz, \quad (47)$$

where $\mathcal{M}_u(z) = \mathcal{E} [e^{-zu}]$ is the MGF of u and $\mathcal{M}_{u,v}(z) = \mathcal{E} [e^{-z(u+v)}]$. Accordingly, (11) can be expressed as $\gamma_{s,k_s}^c = \frac{u}{v + \sigma_{k_s}^2}$ where $u = P_{s,c}x$, $x = \mathbf{g}_{k_s} \mathbf{g}_{k_s}^H$, $v = P_{s,p}y$ and $y = \frac{1}{[(\mathbf{G}_s \mathbf{G}_s^H)^{-1}]_{k_s, k_s}}$. Using (47), the ergodic rate of the common message at the k_s user is

$$\bar{R}_{s,c_{k_s}} = \frac{1}{\ln(2)} \int_0^\infty \frac{1}{z} (1 - \mathcal{M}_u(z)) \mathcal{M}_v(z) e^{-z\sigma_{k_s}^2} dz. \quad (48)$$

Since $\mathbf{g}_{k_s} \sim \mathcal{CN} \left(\sqrt{\frac{\kappa_s}{1+\kappa_s}} \mathbf{h}_{r,k_s}^H \Theta_s \bar{\mathbf{H}}_s, \frac{\kappa_s}{1+\kappa_s} \mathbf{h}_{r,k_s}^H \mathbf{h}_{r,k_s} \right)$, thus $x = \mathbf{g}_{k_s} \mathbf{g}_{k_s}^H$ has Gamma distribution with probability density

function (PDF) given by $f(x) = \frac{(2\nu)^{-\frac{N}{2}}}{\Gamma(\frac{N}{2})} x^{\frac{N}{2}-1} e^{-\frac{x}{2\nu}}$, where $\nu = \frac{1}{1+\kappa_s} \mathbf{h}_{r,k_s}^H \mathbf{h}_{r,k_s} + \frac{\kappa_s}{1+\kappa_s} \mathbf{h}_{r,k_s}^H \Theta_s \bar{\mathbf{H}}_s^H \bar{\mathbf{H}}_s \Theta_s^H \mathbf{h}_{r,k_s}$. Thus, the MGF of x is $\mathcal{M}_x(z) = \mathbb{E} [e^{-zx}] = (1 + 2\nu z)^{-\frac{N}{2}}$. We also know that the PDF of $\zeta = [(\mathbf{G}_s \mathbf{G}_s^H)^{-1}]_{k,k}$ is $f_\zeta(\zeta) = \frac{(\Psi_k)^{N-K+1} e^{-\frac{\Psi_k}{\zeta}}}{\Gamma(N-K+1) \zeta^{(N-K+2)}}$, where Ψ_k is the k th diagonal element of $\Psi_k = \left[\left(\frac{1}{1+\kappa_s} \right) \mathbf{H}_r^H \mathbf{H}_r + \left(\frac{\kappa_s}{1+\kappa_s} \right) \mathbf{H}_r^H \Theta_s \mathbf{a}_M^H \mathbf{a}_M \Theta_s^H \mathbf{H}_r \right]^{-1}_{k_s, k_s}$. Let $y = \frac{1}{\zeta}$, thus the PDF of y is $f_Y(y) = \frac{(\Psi_k)^{N-K+1} y^{(N-K)} e^{-\Psi_k y}}{\Gamma(N-K+1)}$, thus the MGF of y is $\mathcal{M}_Y(z) = (\Psi_k)^{N-K+1} (\Psi_k + z)^{K-N-1}$. By substituting the values of $\mathcal{M}_x(z)$ and $\mathcal{M}_y(z)$ into (48) we can get

$$\begin{aligned} \bar{R}_{s,c_{k_s}} &= \frac{1}{\ln(2)} \int_0^\infty \frac{1}{z} \left(1 - (1 + 2\nu P_{s,c} z)^{-\frac{N}{2}} \right) \\ &\times (\Psi_k)^{N-K+1} (\Psi_k + P_{s,p} z)^{K-N-1} e^{-z\beta} dz. \end{aligned} \quad (49)$$

By Applying Gaussian rules the ergodic common rate in Lemma 1 can be obtained. Now, the ergodic private-rate is

$$\begin{aligned} \mathcal{E} [R_k^p] &= \int_0^\infty \log_2 \left(1 + \frac{P_{s,p} y}{\sigma_{k_s}^2} \right) \\ &\times \frac{y^{(N_s-K)} (\Psi_k)^{N_s-K+1} e^{-\Psi_k y}}{\Gamma(N_s-K+1)} dy. \end{aligned} \quad (50)$$

By applying Gaussian rules the ergodic private rate in Lemma 2 can be obtained.

APPENDIX B

The average SINR of the common message at the k_s^{th} user is

$$\mathcal{E} \{ \gamma_{s,k_s}^c \} = \frac{P_{s,c} \mathcal{E} \{ x \}}{P_{s,p} \mathcal{E} \{ y \} + \sigma_{k_s}^2}, \quad (51)$$

where $x = \frac{\eta_{k_s} \|\mathbf{g}_{k_s}\|^4}{K_s \left(\frac{\kappa_s}{\kappa_s+1} \bar{\mathbf{h}}_{r,k_s}^H \Theta_s \bar{\mathbf{H}}_s^H \Phi_s^H \bar{\mathbf{h}}_{r,k_s} + \frac{N}{\kappa_s+1} M \right)}$ and $y = \frac{1}{[(\mathbf{G}_s \mathbf{G}_s^H)^{-1}]_{k_s, k_s}}$. Now, the average of x can be evaluated by,

$$\mathcal{E} \{ x \} = \eta_{k_s} \mathcal{E} \left\{ \left\| \mathbf{h}_{r,k_s}^H \Theta_s \mathbf{H}_s \mathbf{H}_s^H \Theta_s^H \mathbf{h}_{r,k_s} \right\|^2 \right\} \quad (52)$$

where

$$\begin{aligned} \mathbf{h}_{r,k_s}^H \Theta_s \mathbf{H}_s \mathbf{H}_s^H \Theta_s^H \mathbf{h}_{r,k_s} &= \mathbf{h}_{r,k}^H \Theta_s \left(\frac{\kappa_s}{\kappa_s+1} \bar{\mathbf{H}} \bar{\mathbf{H}}^H + \right. \\ &\left. \frac{\sqrt{\kappa_s}}{\kappa_s+1} \tilde{\mathbf{H}} \tilde{\mathbf{H}}^H + \frac{\sqrt{\kappa_s}}{\kappa_s+1} \tilde{\mathbf{H}} \tilde{\mathbf{H}}^H + \frac{1}{\kappa_s+1} \tilde{\mathbf{H}} \tilde{\mathbf{H}}^H \right) \Theta_s^H \mathbf{h}_{r,k_s} \\ &= \frac{1}{\kappa_s+1} \mathbf{h}_{r,k}^H \Theta_s \left(\kappa_s \bar{\mathbf{H}} \bar{\mathbf{H}}^H + \sqrt{\kappa_s} \tilde{\mathbf{H}} \tilde{\mathbf{H}}^H \right. \\ &\left. + \sqrt{\kappa_s} \tilde{\mathbf{H}} \tilde{\mathbf{H}}^H + \tilde{\mathbf{H}} \tilde{\mathbf{H}}^H \right) \Theta_s^H \mathbf{h}_{r,k_s} = \frac{1}{\kappa_s+1} \mathbf{h}_{r,k}^H \mathbf{A} \mathbf{h}_{r,k} \end{aligned} \quad (53)$$

where

$$\mathbf{A} = \Theta_s \left(\kappa_s \bar{\mathbf{H}}\bar{\mathbf{H}}^H + \sqrt{\kappa_s} \bar{\mathbf{H}}\tilde{\mathbf{H}}^H + \sqrt{\kappa_s} \tilde{\mathbf{H}}\bar{\mathbf{H}}^H + \tilde{\mathbf{H}}\tilde{\mathbf{H}}^H \right) \Theta_s^H.$$

Now (53) can be expressed as $\frac{1}{\kappa_s+1} \mathbf{h}_{r,k}^H \mathbf{A} \mathbf{h}_{r,k} = \frac{1}{\kappa_s+1} \underbrace{\bar{\mathbf{h}}_{r,k}^H \mathbf{A} \bar{\mathbf{h}}_{r,k}}_{\Delta_1}$. After removing the zero expectation terms, we can get

$$\mathcal{E} \left\{ |\mathbf{h}_{r,k}^H \Theta_s \mathbf{H}_s \mathbf{H}_s^H \Theta_s^H \mathbf{h}_{r,k}|^2 \right\} = \frac{1}{(\kappa_s+1)^2} \mathcal{E} \left\{ |\Delta_1|^2 \right\}. \quad (54)$$

Now we can write the main term as

$$\Delta_1 = \frac{1}{\kappa_s+1} \bar{\mathbf{h}}_{r,k}^H \Theta_s \left(\kappa_s \bar{\mathbf{H}}\bar{\mathbf{H}}^H + \sqrt{\kappa_s} \bar{\mathbf{H}}\tilde{\mathbf{H}}^H + \sqrt{\kappa_s} \tilde{\mathbf{H}}\bar{\mathbf{H}}^H + \tilde{\mathbf{H}}\tilde{\mathbf{H}}^H \right) \Theta_s^H \bar{\mathbf{h}}_{r,k} \quad (55)$$

$$= \left(\underbrace{\frac{\kappa_s}{\kappa_s+1} \bar{\mathbf{h}}_{r,k}^H \Theta_s \bar{\mathbf{H}}\bar{\mathbf{H}}^H \Theta_s^H \bar{\mathbf{h}}_{r,k}}_{\Delta_{1,1}} + \underbrace{\frac{\sqrt{\kappa_s}}{\kappa_s+1} \bar{\mathbf{h}}_{r,k}^H \Theta_s \bar{\mathbf{H}}\tilde{\mathbf{H}}^H \Theta_s^H \bar{\mathbf{h}}_{r,k}}_{\Delta_{1,2}} + \underbrace{\frac{\sqrt{\kappa_s}}{\kappa_s+1} \bar{\mathbf{h}}_{r,k}^H \Theta_s \tilde{\mathbf{H}}\bar{\mathbf{H}}^H \Theta_s^H \bar{\mathbf{h}}_{r,k}}_{\Delta_{1,3}} + \underbrace{\frac{1}{\kappa_s+1} \bar{\mathbf{h}}_{r,k}^H \Theta_s \tilde{\mathbf{H}}\tilde{\mathbf{H}}^H \Theta_s^H \bar{\mathbf{h}}_{r,k}}_{\Delta_{1,4}} \right). \quad (56)$$

The average can be extended into

$$\mathcal{E} \left\{ |\Delta_1|^2 \right\} = \mathcal{E} \left\{ |\Delta_{1,1}|^2 \right\} + \mathcal{E} \left\{ |\Delta_{1,2}|^2 \right\} + \mathcal{E} \left\{ |\Delta_{1,3}|^2 \right\} + \mathcal{E} \left\{ |\Delta_{1,4}|^2 \right\} + 2\mathcal{E} \left\{ \Delta_{1,1}\Delta_{1,4}^* \right\}. \quad (57)$$

The average of the first term is

$$\mathcal{E} \left\{ |\Delta_{1,1}|^2 \right\} = \left(\frac{\kappa_s}{\kappa_s+1} \right)^2 \left(|\bar{\mathbf{h}}_{r,k}^H \Theta_s \bar{\mathbf{H}}\bar{\mathbf{H}}^H \Theta_s^H \bar{\mathbf{h}}_{r,k}|^2 \right). \quad (58)$$

and the average of the second term is

$$\mathcal{E} \left\{ |\Delta_{1,2}|^2 \right\} = \frac{\kappa_s}{(\kappa_s+1)^2} NM |f_k|^2 \quad (59)$$

where, $f_k = \mathbf{a}_N(\phi_r^a, \phi_r^e) \Theta_s \bar{\mathbf{h}}_{r,k}^H$. The average of the third term is

$$\mathcal{E} \left\{ |\Delta_{1,3}|^2 \right\} = \frac{\kappa_s}{(\kappa_s+1)^2} (NM |f_k|^2). \quad (60)$$

The average of the fourth term

$$\mathcal{E} \left\{ |\Delta_{1,4}|^2 \right\} = \frac{1}{(\kappa_s+1)^2} (N^2 M^2 + NM^2). \quad (61)$$

The average of the last term is

$$2\mathcal{E} \left\{ \Delta_{1,1}\Delta_{1,4}^* \right\} = 2 \frac{\kappa_s}{(\kappa_s+1)^2} \bar{\mathbf{h}}_{r,k}^H \Theta_s \bar{\mathbf{H}}\bar{\mathbf{H}}^H \Theta_s^H \bar{\mathbf{h}}_{r,k} \bar{\mathbf{h}}_{r,k}^H \mathbf{N} \mathbf{I}_M \bar{\mathbf{h}}_{r,k}. \quad (62)$$

Now, we need to find the expectation of y , $\mathcal{E} \{y\} = \mathcal{E} \left\{ \frac{1}{[(\mathbf{G}_s \mathbf{G}_s^H)^{-1}]_{k_s, k_s}} \right\}$. Since $\mathbf{G}_s \mathbf{G}_s^H$ has wishart distribution, we know that

$$\mathcal{E} \left\{ \mathbf{G}_s \mathbf{G}_s^H \right\} = N \left(\left(\frac{1}{1+\kappa_s} \right) \mathbf{H}_r^H \mathbf{H}_r + \right.$$

$$\left. \left(\frac{\kappa_s}{1+\kappa_s} \right) \mathbf{H}_r^H \Theta_s \mathbf{a}_M^H \mathbf{a}_M \Theta_s^H \mathbf{H}_r \right). \quad (63)$$

Thus the expectation can be found as

$$\mathcal{E} \left\{ (\mathbf{G}_s \mathbf{G}_s^H)^{-1} \right\} = \frac{1}{N-K-1} \left(\left(\frac{1}{1+\kappa_s} \right) \mathbf{H}_r^H \mathbf{H}_r + \left(\frac{\kappa_s}{1+\kappa_s} \right) \mathbf{H}_r^H \Theta_s \mathbf{a}_M^H \mathbf{a}_M \Theta_s^H \mathbf{H}_r \right)^{-1}. \quad (64)$$

Finally, by substituting $\mathcal{E} \{x\}$ and $\mathcal{E} \{y\}$ in (51) we can obtain the ergodic rate for the common message. Similarly, by plugging $\mathcal{E} \{y\}$ into (19) we can get the ergodic rate of the private part.

APPENDIX C

Based on the Woodbury's identity, we have

$$\left[(\Lambda + \delta \mathbf{H}_r^H \Theta_s \mathbf{a}_M^H \mathbf{a}_M \Theta_s^H \mathbf{H}_r)^{-1} \right]_{k_s, k_s} = \left[\Lambda^{-1} \right]_{k_s, k_s} - \frac{\delta \left[\Lambda^{-1} \mathbf{H}_r^H \Theta_s \mathbf{a}_M^H \mathbf{a}_M \Theta_s^H \mathbf{H}_r \Lambda^{-1} \right]_{k_s, k_s}}{1 + \delta \mathbf{a}_M^H \Theta_s^H \mathbf{H}_r \Lambda^{-1} \mathbf{H}_r^H \Theta_s \mathbf{a}_M^H} \quad (65)$$

where $\Lambda = \left(\frac{1}{1+\kappa_s} \right) \mathbf{H}_r^H \mathbf{H}_r$ and $\delta = \left(\frac{\kappa_s}{1+\kappa_s} \right)$. Now using $\Theta_s \mathbf{a}_M^H = \text{diag}(\mathbf{a}_M^H) \theta_s$, we can get (66), where $\mathbf{B}_{k_s} = \left(\frac{1}{M} \mathbf{I}_M + \delta \text{diag}(\mathbf{a}_M) \mathbf{H}_r \Lambda^{-1} \mathbf{H}_r^H \text{diag}(\mathbf{a}_M^H) \right)$, $\mathbf{s} = \left[\Lambda^{-1} \mathbf{H}_r^H \text{diag}(\mathbf{a}_M^H) \right]_{(:,k)}$, $\mathbf{s}^H = \left[\Lambda^{-1} \mathbf{H}_r^H \text{diag}(\mathbf{a}_M^H) \right]_{(k,:)}$ and $\mathbf{A}_{k_s} = \left\{ \left[\Lambda^{-1} \right]_{k_s, k_s} \mathbf{B}_{k_s} - \delta \mathbf{s} \mathbf{s}^H \right\}$.

REFERENCES

- [1] D. Jun, W. Ham, J.-Y. Kwon, C.-B. Chae, and R. W. Heath Jr., "Reconfigurable intelligence surface with potential tunable meta-devices for 6G: Design and system-level evaluation," *IEEE Communications Standard Magazine*, 2024.
- [2] L. Dai, B. Wang, M. Wang, X. Yang, J. Tan, S. Bi, S. Xu, F. Yang, Z. Chen, M. D. Renzo, C.-B. Chae, and L. Hanzo, "Reconfigurable intelligent surface-based wireless communications: Antenna design, prototyping, and experimental results," *IEEE Access*, vol. 8, no. 1, pp. 45 913–45 923, 2020.
- [3] A. Salem, K.-K. Wong, C.-B. Chae, and Y. Zhang, "Star-ris assisted full-duplex communication networks," 2023. [Online]. Available: <https://arxiv.org/abs/2309.15037>
- [4] —, "User clustering for star-ris assisted full-duplex noma communication systems," 2023. [Online]. Available: <https://arxiv.org/abs/2401.00447>
- [5] M. Di Renzo, A. Zappone, M. Debbah, M.-S. Alouini, C. Yuen, J. de Rosny, and S. Tretyakov, "Smart radio environments empowered by reconfigurable intelligent surfaces: How it works, state of research, and the road ahead," *IEEE Journal on Selected Areas in Communications*, vol. 38, no. 11, pp. 2450–2525, 2020.
- [6] Q. Wu and R. Zhang, "Intelligent reflecting surface enhanced wireless network via joint active and passive beamforming," *IEEE Transactions on Wireless Communications*, vol. 18, no. 11, pp. 5394–5409, 2019.
- [7] C. Huang, A. Zappone, G. C. Alexandropoulos, M. Debbah, and C. Yuen, "Reconfigurable intelligent surfaces for energy efficiency in wireless communication," *IEEE Transactions on Wireless Communications*, vol. 18, no. 8, pp. 4157–4170, 2019.
- [8] S. Zhang and R. Zhang, "Capacity characterization for intelligent reflecting surface aided MIMO communication," *IEEE Journal on Selected Areas in Communications*, vol. 38, no. 8, pp. 1823–1838, 2020.
- [9] Q. Tao, J. Wang, and C. Zhong, "Performance analysis of intelligent reflecting surface aided communication systems," *IEEE Communications Letters*, vol. 24, no. 11, pp. 2464–2468, 2020.

$$\begin{aligned}
& [\Lambda^{-1}]_{k_s, k_s} - \frac{\delta \left[\Lambda^{-1} \mathbf{H}_r^H \text{diag}(\mathbf{a}_M^H) \theta_s \theta_s^H \text{diag}(\mathbf{a}_M) \mathbf{H}_r \Lambda^{-1} \right]_{k_s, k_s}}{1 + \delta \theta_s^H \text{diag}(\mathbf{a}_M) \mathbf{H}_r \Lambda^{-1} \mathbf{H}_r^H \text{diag}(\mathbf{a}_M^H) \theta_s} = \\
& [\Lambda^{-1}]_{k_s, k_s} - \frac{\delta \left[\Lambda^{-1} \mathbf{H}_r^H \text{diag}(\mathbf{a}_M^H) \theta_s \theta_s^H \text{diag}(\mathbf{a}_M) \mathbf{H}_r \Lambda^{-1} \right]_{k_s, k_s}}{\frac{1}{M} \theta_s^H \mathbf{I}_M \theta_s + \delta \theta_s^H \text{diag}(\mathbf{a}_M) \mathbf{H}_r \Lambda^{-1} \mathbf{H}_r^H \text{diag}(\mathbf{a}_M^H) \theta_s} = \\
& [\Lambda^{-1}]_{k_s, k_s} - \frac{\delta \left[\Lambda^{-1} \mathbf{H}_r^H \text{diag}(\mathbf{a}_M^H) \theta_s \theta_s^H \text{diag}(\mathbf{a}_M) \mathbf{H}_r \Lambda^{-1} \right]_{k_s, k_s}}{\theta_s^H \left(\frac{1}{M} \mathbf{I}_M + \delta \text{diag}(\mathbf{a}_M) \mathbf{H}_r \Lambda^{-1} \mathbf{H}_r^H \text{diag}(\mathbf{a}_M^H) \right) \theta_s} = \frac{\theta_s^H \left\{ [\Lambda^{-1}]_{k_s, k_s} \mathbf{B}_{k_s} - \delta \mathbf{ss}^H \right\} \theta_s}{\theta_s^H \mathbf{B}_{k_s} \theta_s} = \frac{\theta_s^H \mathbf{A}_{k_s} \theta_s}{\theta_s^H \mathbf{B}_{k_s} \theta_s} \quad (66)
\end{aligned}$$

- [10] W. Tang, M. Z. Chen, X. Chen, J. Y. Dai, Y. Han, M. Di Renzo, Y. Zeng, S. Jin, Q. Cheng, and T. J. Cui, "Wireless communications with reconfigurable intelligent surface: Path loss modeling and experimental measurement," *IEEE Transactions on Wireless Communications*, vol. 20, no. 1, pp. 421–439, 2021.
- [11] T. Bai, C. Pan, Y. Deng, M. Elkhshlan, A. Nallanathan, and L. Hanzo, "Latency minimization for intelligent reflecting surface aided mobile edge computing," *IEEE Journal on Selected Areas in Communications*, vol. 38, no. 11, pp. 2666–2682, 2020.
- [12] K. Zhi, C. Pan, H. Ren, K. Wang, M. Elkhshlan, M. D. Renzo, R. Schober, H. V. Poor, J. Wang, and L. Hanzo, "Two-timescale design for reconfigurable intelligent surface-aided massive mimo systems with imperfect csi," *IEEE Transactions on Information Theory*, vol. 69, no. 5, pp. 3001–3033, 2023.
- [13] J. Zhang, J. Liu, S. Ma, C.-K. Wen, and S. Jin, "Large system achievable rate analysis of RIS-assisted MIMO wireless communication with statistical CSIT," *IEEE Transactions on Wireless Communications*, vol. 20, no. 9, pp. 5572–5585, 2021.
- [14] K. Xu, J. Zhang, X. Yang, S. Ma, and G. Yang, "On the sum-rate of RIS-assisted MIMO multiple-access channels over spatially correlated rician fading," *IEEE Transactions on Communications*, vol. 69, no. 12, pp. 8228–8241, 2021.
- [15] K. Zhi, C. Pan, H. Ren, and K. Wang, "Ergodic rate analysis of reconfigurable intelligent surface-aided massive MIMO systems with ZF detectors," *IEEE Communications Letters*, vol. 26, no. 2, pp. 264–268, 2022.
- [16] M. Abbasi Mosleh, F. Heliot, and R. Tafazolli, "Ergodic capacity analysis of reconfigurable intelligent surface assisted MIMO systems over Rayleigh-Rician channels," *IEEE Communications Letters*, pp. 1–1, 2022.
- [17] Z. Li, M. Hua, Q. Wang, and Q. Song, "Weighted sum-rate maximization for multi-irs aided cooperative transmission," *IEEE Wireless Communications Letters*, vol. 9, no. 10, pp. 1620–1624, 2020.
- [18] H. Guo, Y.-C. Liang, J. Chen, and E. G. Larsson, "Weighted sum-rate maximization for reconfigurable intelligent surface aided wireless networks," *IEEE Transactions on Wireless Communications*, vol. 19, no. 5, pp. 3064–3076, 2020.
- [19] M.-A. Badiu and J. P. Coon, "Communication through a large reflecting surface with phase errors," *IEEE Wireless Communications Letters*, vol. 9, no. 2, pp. 184–188, 2020.
- [20] A. Salem, K.-K. Wong, and C.-B. Chae, "Impact of phase-shift error on the secrecy performance of uplink RIS communication systems," *IEEE Transactions on Wireless Communications*, pp. 1–1, 2023.
- [21] B. Clerckx, H. Joudeh, C. Hao, M. Dai, and B. Rassouli, "Rate splitting for mimo wireless networks: a promising phy-layer strategy for lte evolution," *IEEE Communications Magazine*, vol. 54, no. 5, pp. 98–105, May 2016.
- [22] A. S. de Sena, P. H. J. Nardelli, D. B. da Costa, P. Popovski, and C. B. Papadias, "Rate-splitting multiple access and its interplay with intelligent reflecting surfaces," *IEEE Communications Magazine*, vol. 60, no. 7, pp. 52–57, 2022.
- [23] M. Katwe, K. Singh, B. Clerckx, and C.-P. Li, "Rate splitting multiple access for sum-rate maximization in irs aided uplink communications," *IEEE Transactions on Wireless Communications*, vol. 22, no. 4, pp. 2246–2261, 2023.
- [24] A. Bansal, K. Singh, B. Clerckx, C.-P. Li, and M.-S. Alouini, "Rate-splitting multiple access for intelligent reflecting surface aided multi-user communications," *IEEE Transactions on Vehicular Technology*, vol. 70, no. 9, pp. 9217–9229, 2021.
- [25] S. Pala, M. Katwe, K. Singh, B. Clerckx, and C.-P. Li, "Spectral-efficient ris-aided rsma urlhc: Toward mobile broadband reliable low latency communication (mbrllc) system," *IEEE Transactions on Wireless Communications*, vol. 23, no. 4, pp. 3507–3524, 2024.
- [26] B. Li, W. Chen, Z. Li, Q. Wu, N. Cheng, C. Li, and L. Dai, "Robust weighted sum-rate maximization for transmissive ris transmitter enabled rsma networks," *IEEE Communications Letters*, vol. 27, no. 10, pp. 2847–2851, 2023.
- [27] H. Li, Y. Mao, O. Dizdar, and B. Clerckx, "Rate splitting multiple access for 6G Part-III: Interplay with reconfigurable intelligent surfaces," *IEEE Communications Letters*, vol. 26, no. 10, pp. 2242–2246, 2022.
- [28] W. Cai, H. Li, M. Li, and Q. Liu, "Practical modeling and beamforming for intelligent reflecting surface aided wideband systems," *IEEE Communications Letters*, vol. 24, no. 7, pp. 1568–1571, 2020.
- [29] H. Li, W. Cai, Y. Liu, M. Li, Q. Liu, and Q. Wu, "Intelligent reflecting surface enhanced wideband mimo-ofdm communications: From practical model to reflection optimization," *IEEE Transactions on Communications*, vol. 69, no. 7, pp. 4807–4820, 2021.
- [30] W. Cai, R. Liu, M. Li, Y. Liu, Q. Wu, and Q. Liu, "IRS-assisted multicell multiband systems: Practical reflection model and joint beamforming design," *IEEE Transactions on Communications*, vol. 70, no. 6, pp. 3897–3911, 2022.
- [31] S. Liu, R. Liu, M. Li, Y. Liu, and Q. Liu, "Joint BS-RIS-user association and beamforming design for RIS-assisted cellular networks," *IEEE Transactions on Vehicular Technology*, vol. 72, no. 5, pp. 6113–6128, 2023.
- [32] K. Zhi, C. Pan, G. Zhou, H. Ren, M. Elkhshlan, and R. Schober, "Is ris-aided massive mimo promising with zf detectors and imperfect csi?" *IEEE Journal on Selected Areas in Communications*, vol. 40, no. 10, pp. 3010–3026, 2022.
- [33] G. Xiao, T. Yang, C. Huang, X. Wu, H. Feng, and B. Hu, "Average rate approximation and maximization for RIS-assisted multi-user MISO system," *IEEE Wireless Communications Letters*, vol. 11, no. 1, pp. 173–177, 2022.
- [34] B. Zheng, C. You, and R. Zhang, "Intelligent reflecting surface assisted multi-user ofdma: Channel estimation and training design," *IEEE Transactions on Wireless Communications*, vol. 19, no. 12, pp. 8315–8329, 2020.
- [35] M. Abramowitz and I. A. Stegun, *Handbook of Mathematical Functions With Formulas, Graphs, and Mathematical Tabl*, Washington, D.C.: U.S. Dept. Commerce, 1972.
- [36] K. Shen and W. Yu, "Fractional programming for communication systems part I: Power control and beamforming," *IEEE Transactions on Signal Processing*, vol. 66, no. 10, pp. 2616–2630, 2018.
- [37] —, "Fractional programming for communication systems part II: Uplink scheduling via matching," *IEEE Transactions on Signal Processing*, vol. 66, no. 10, pp. 2631–2644, 2018.
- [38] M. Dai, B. Clerckx, D. Gesbert, and G. Caire, "A rate splitting strategy for massive MIMO with imperfect CSIT," *IEEE Transactions on Wireless Communications*, vol. 15, no. 7, pp. 4611–4624, 2016.
- [39] K. Hamdi, "A useful lemma for capacity analysis of fading interference channels," *IEEE Trans. Commun.*, vol. 58, no. 2, pp. 411–416, Feb. 2010.